CFD SIMULATIONS OF VENTILATION EFFECT ON HYDROGEN RELEASE BEHAVIOR AND COMBUSTION IN AN UNDERGROUND MINING ENVIRONMENT

ABSTRACT

CFD simulations investigating the effect of ventilation airflow on hydrogen release behavior in an underground mining tunnel were performed using FLACS hydrogen. Both dispersion and combustion scenarios of a hydrogen release coming from a severed distribution pipeline were investigated. Effects on the hydrogen dispersion such as ventilation strength and the mechanism of air flow supply (a "pull" or "push" fan) and mine opening surface roughness, surface cavities and obstructions were explored. Results showing the effect of changing the position of the leak, adding a cavity on the ceiling of the tunnel and changing the roughness of the walls are given. Overpressure sensitivity to the ignition delay was also considered. From the results, for the varied ventilation regimes and spatial scenarios, it is difficult to identify the optimal ventilation strategy giving the safest conditions for hydrogen distribution and refueling in an underground mine.

1.0 INTRODUCTION

The use of hydrogen as an energy carrier for routine underground mining application is not new, in the 1980's it was the subject of U.S. Bureau of Mines research program into alternative power sources [1]. Since 2000 there has been renewed interest in North America to use hydrogen power underground and it has been the subject of several proof-of-concept projects, including power plant design, retrofitting and testing of fuel cell powered mine vehicles and the recommendation to apply conventional hydrogen storage and distribution infrastructure to underground refuelling needs. The impetus behind this thrust is to provide the mining industry with a cleaner power source for their primary production vehicles. As covered previously [2, 3] fuel cell powered vehicles have the potential to reduce the demand for ventilation where they replace diesel equipment, a primary ventilation volume design criteria. Hydrogen powered vehicles could also help offset any increased need for ventilation as health regulations pertaining to the exposure of workers to diesel particulate matter become more demanding. This type of vehicle could also produce less heat and help the industry to reduce its environmental footprint through lower greenhouse gas emissions not only from the mobile vehicle but also from the ventilation system.

In this work, computational fluid dynamics (CFD) modeling was undertaken to investigate the effect of the ventilation airflow turbulence on hydrogen release behavior in underground mining environment depending on the strength and direction of air flow (pull and push), space geometries, surface roughness, surface cavities and obstructions. Combustion results and overpressure sensitivity to the ignition delay were also investigated.

2.0 METHODOLOGY

The simulations were performed using the commercial CFD code FLACS/Hydrogen from GexCon. The conservation equations for mass, momentum, and enthalpy in addition to conservation equations for concentration, are solved on a structured grid using a finite volume method. The SIMPLE pressure-velocity correction method is used and extended for compressible flows with source terms for the compression work in the enthalpy equation. FLACS uses the k-ε turbulent model and the ideal gas equation of state. The combustion model used in FLACS is an effective flame velocity approach which assumes a one-step reaction scheme and relies on a three-part burning velocity model and a flame folding model. Sub-grid objects are modeled using a porosity approach.

For jet dispersion cases, when the flow is choked at the jet exit, the jet outlet conditions, i.e. the leak rate, temperature, effective leak area, velocity and the turbulence parameters (turbulence intensity and turbulent length scale) for the flow, are calculated using an embedded jet program in the FLACS

package. FLACS can also calculate the time dependent leak and turbulence parameter data for continuous jet releases in the case of high pressure vessel depressurization. The estimation assumes isentropic flow conditions through the nozzle, followed by a single normal shock (whose properties are calculated using the Rankine-Hugoniot relations), which is subsequently followed by expansion into ambient air [4].

FLACS has been extensively validated against experimental data and reasonable agreement was seen for hydrogen dispersion simulations for various release conditions [5] as well as for hydrogen deflagration in a tunnel [6]. Hydrogen leak dispersion followed by subsequent gas explosions simulations were also validated against experiments [7]. Short and long term distribution and mixing of hydrogen in a close environment were also validated [8][9] as well as the influence of wind (ventilation) on hydrogen release [10].

FLACS uses a rectilinear grid. In the case of jet dispersion, a refined zone made of cubic cells is defined at the expanded jet location. Following Gexcon good practice recommendations [11], the cell size of the refined cubic zone at the expanded jet location is determined by the effective leak area A_{leak} so that $A_{cv} > A_{leak} > 0.9A_{cv}$ where A_{cv} is the area of the control volume face. The leak originates from one cell in the refined cubic zone. From that refined zone, the grid is stretched to a coarser 0.1 m cubic grid. In the case of "after leak" dispersions as well as combustion simulations, jet dispersion results were imported onto a uniform 0.1 m cubic grid devoid of any cell refinement around the leak origin.

3.0 MODELING DOMAIN AND ASSUMPTIONS

The mine opening is represented by a rectangular tunnel 2.6 m wide, 2.7 m high and 30 m long as shown in Figure 1. The roughness of the walls and ceiling is modeled using a 0.1 m thick porous region with a porosity of 95% (5% blockage). The leak opening is set at X = 0.20 m, Y = 1.30 m and Z = 1.35 m in the middle of the wall. A 0.61 m x 0.61 m (2'x2') exhaust fan opening is positioned above the leak point. For dispersion cases, with no ventilation, the outer wall is porous at 5 % (95% blockage) whereas it is fully open for the ventilation scenarios. For all combustion cases the outer wall is porous at 5 % (95% blockage). A mine opening with dimensions of 3.7 m wide, 4.0 m high and 30 m long was also considered. These cross-sectional areas are considered typical dimensions for larger scale and smaller scale mining respectively.

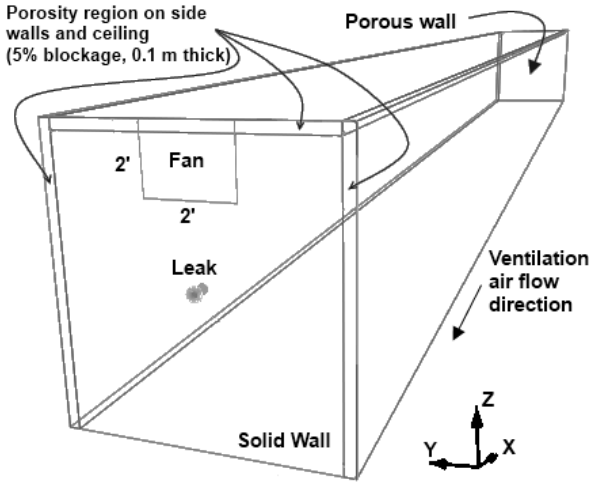

Figure 1. Mine opening schematics and “pull” ventilation arrangements.

The horizontal leak is assumed to originate from a ruptured pipeline with an internal diameter of 8.48 mm. The hydrogen is released from a 100 kg storage tank at 300 psi (20.684 bar). While three leak diameters (8.48 mm (full leak), 4.24 mm (half leak) and 2.63 mm (small leak)) and three release durations (1 second, 3 seconds and full uncontrolled release) were considered during the study, only one of each is presented in this paper: d = 8.48 mm (full leak), 3 seconds release. The initial mass flow

rate of the full leak is 0.073 kg/s. These values were chosen to represent the worst possible leak conditions from an industrial accident, taking into consideration the capability of pressure sensing and shut-down delivery safety systems.

Both “pull” and “push” ventilation scenarios are considered with a fan exhausting from or forcing into the refueling area. The ventilation is provided by fan in a 0.61 m x 0.61 m opening positioned either right above the leak for the “pull” ventilation set-up (Figure 1), or blowing into the tunnel far end for the “push” ventilation scenario. In both cases, the ventilation was directed against the leak (against the x-axis). The average air velocities considered transiting through the mine tunnel were of 0.5 m/s and 3 m/s. These were respectively considered a minimal requirement for support activities underground and an average value for active mine production conditions.

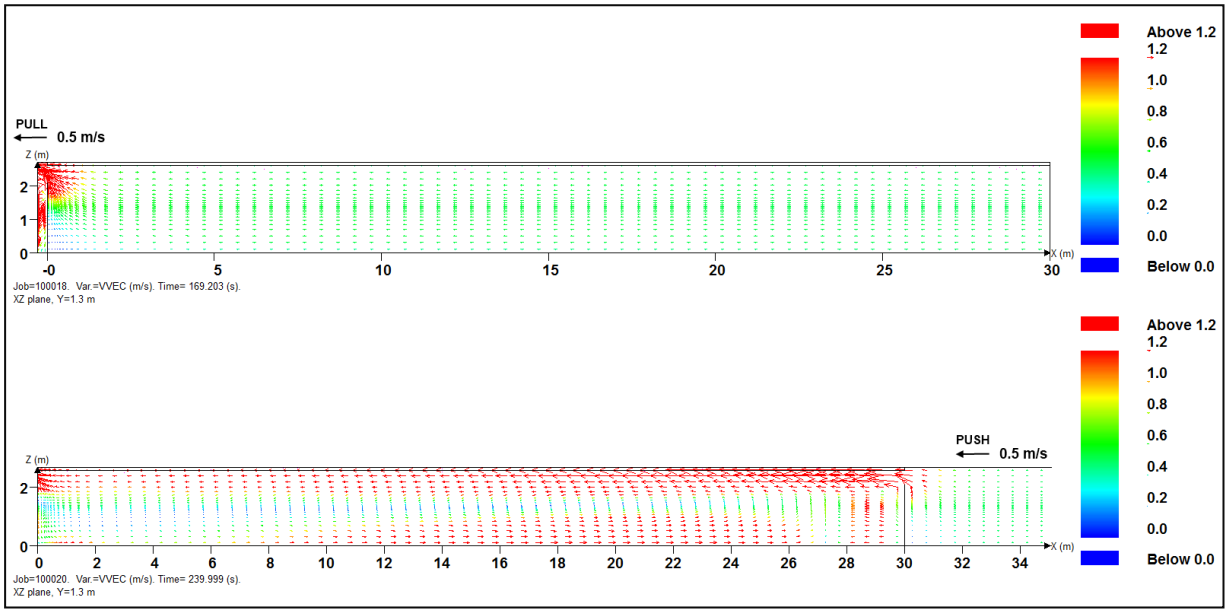

Figure 2. 0.5 m/s “pull” and “push” ventilation velocity field on the plane in the center of the domain (y = 1.3m)

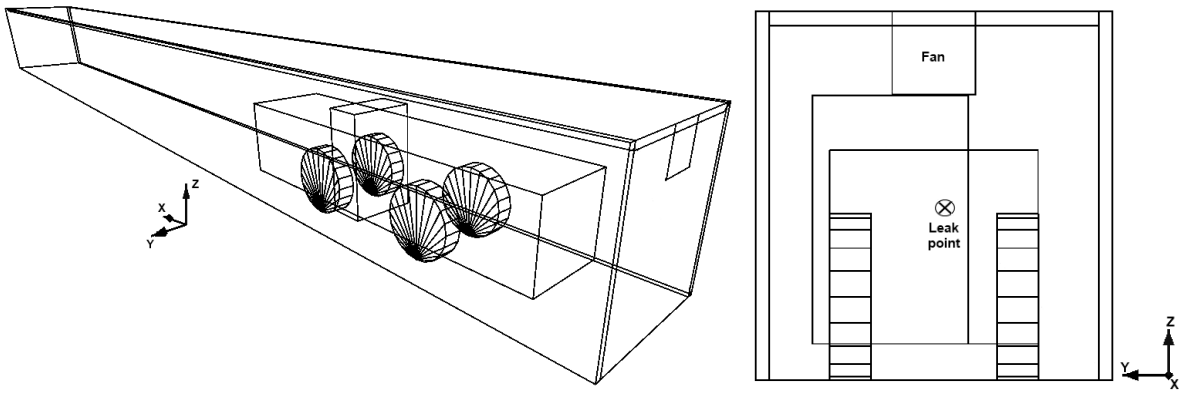

Figure 3. Isometric and back view of the tunnel with an underground loader placed 1 m away from the leak origin.

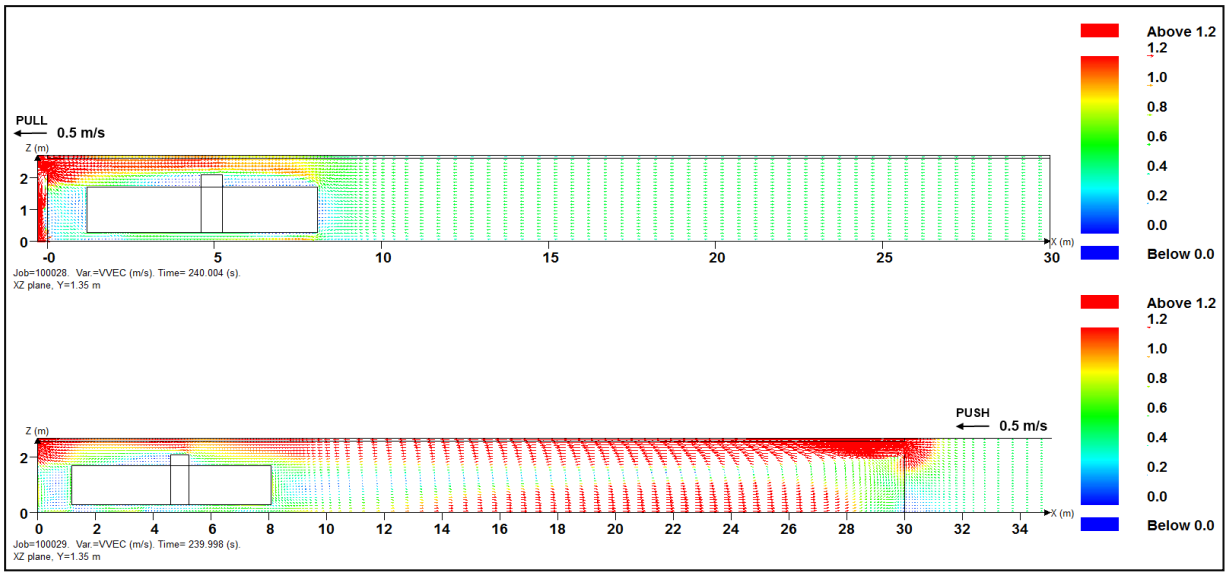

Figure 4. 0.5 m/s "pull" and "push" ventilation velocity field on the plane in the center of the domain (y = 1.3 m) in the presence of a vehicle

The ventilation velocity is assumed to correspond to the average velocity in the domain. To correctly simulate the velocity field inside the tunnel, the domain is extended beyond the fan opening by 0.3 m in the case of the "pull" ventilation and by 5 m in the case of the "push" ventilation. Results for the 0.5 m/s average air velocity are presented in this paper for the worst case scenario. Figure 2 illustrates the 0.5 m/s velocity profiles in the middle of the simulation domain (Y = 1.3 m) for both the "pull" and "push" ventilation scenarios. Notable in this figure is that under the "pull" scenario the velocity vectors all show a common orientation towards the fan. Whereas under the "push" ventilation scenario, although the high velocity discharge from the fan (upper right) entrains additional flow towards the discharge, this local enhancement of the flow in the upper section of the tunnel comes at the cost of a flow reversal in the lower section of the tunnel.

For the smaller mine opening considering an obstacle, a vehicle is added at a distance of 1 m from the leak location. An Atlas Copco underground loader (EST2D) is used as the basis for the obstacle dimensions. For modeling purposes, a simplified representation of the vehicle is used as shown in Figure 3. The operator's cab is assumed to be enclosed. Figure 4 shows the 0.5 m/s "pull" and "push" ventilation generated velocity vector profiles resulting from the presence of the loader. As may be expected the loader creates a higher velocity zone, above the loader immediately ahead of the tunnel discharge regardless of the ventilation scenario. For the "push" ventilation condition a similar flow reversal effect is generated, but as a whole the volume in which the high velocity contours exist is condensed.

4.0 DISPERSION RESULTS: THE EFFECT OF "PULL" AND "PUSH" VENTILATION

The dispersion simulations were performed in two stages. First the hydrogen is released in the domain for 3 seconds, then the release is stopped and the hydrogen is allowed to dissipate until there is no more hydrogen above a 4% molar fraction (the lower flammability limit or LFL) present in the simulation domain. These were performed for both tunnel cross-sectional areas, and for the smaller tunnel with the loader obstruction. Results were also obtained for three other scenarios in the smaller cross-section. In the first one the leak position is lowered from z = 1.35 m centerline to a position closer to the ground at z = 0.25 m. For the second scenario a 1 m deep, 2 m long, 2.6 m wide cavity is added on the ceiling at x = 8 m. In the last scenario, the 95% porous region on the wall is replaced with a series of rectangular boxes of the same depth and width as the simulation grid (0.1 m). Each rectangular box is separated from the next by a random distance varying between 0.1 m and 0.7 m.

Table 1 summarizes the results of thirteen modeling runs across the six geometric scenarios. Three ventilation states, no ventilation, a “pull” fan and a “push” are given for the default small tunnel, but this is reduced to only the no ventilation and “pull” fan conditions for the remaining considerations. This table shows the minimum and maximum 4% mole fraction extents of the hydrogen cloud inside the mine opening for each scenario. In the same table, the time it takes for the 4% molar fraction hydrogen cloud to completely dissipate is also given. The minimum and maximum extents represent the minimum and maximum distances at which the concentration level of hydrogen reaches the threshold of 4% (by volume) along the specified axis. Still images at selected time steps showing a planar cut passing through the center of the tunnel along the x-axis (XZ plane in the middle of the domain, corresponding to a transverse cut of the simulation domain) are also shown in Figure 5 and Figure 6.

In the case of an empty tunnel (Figure 5), the “pull” ventilation yields a slightly longer extent and size cloud than the “push” ventilation. On the other hand the behavior of the cloud is a lot more erratic with the “push” ventilation than with the “pull”, this is more evident in the dynamic visualization offered by the CFD modeling. The turbulent air flow generated by the “push” ventilation dissipates the hydrogen cloud more rapidly inside the tunnel when compared to the less turbulent air flow induced by the “pull” ventilation which purges hydrogen outside the mine opening. Figure 5 also shows how the 4 % mole fraction contour is affected by a 0.5 m/s average velocity versus the zero airflow régime. For both ventilation types, “push” and “pull”, the lower concentration region of the hydrogen cloud is being drawn or forced back inside the higher concentration part of the cloud. This effect raises the overall concentration of the cloud in the vicinity of the release point which would lead to higher overpressures from an ignition, as shown in the next section. However in terms of dispersion rates, Table 1 shows “push” ventilation to be most effective, while “pull” ventilation is only slightly better than no ventilation for the short duration leak.

Table 1 also shows the effect of tunnel size, when it is increased the time required to completely dissipate the cloud diminishes quite significantly going from 76.4 sec to 12.7 sec with “pull” ventilation; hence, small volume mine opening being considered the worst case for a specific size leak.

Table 1. Minimum and maximum 4% mole fraction extents at 3 sec and during "after-leaks" dispersion for the full leak scenarios. The time it takes for the 4% molar fraction cloud to completely dissipate is also given.

Scenario		Minimum and maximum 4% mole fraction extents (in m)												
		At 3 seconds						After-leaks dispersion						
		X_{min}	$\mathbf{X_{max}}$	Y_{min}	Y_{max}	Z_{min}	Z_{max}	X_{min}	$\mathbf{X_{max}}$	Y_{min}	Y_{max}	Z_{min}	Z_{max}	**Time (sec)**
Default Tunnel	No vent.	0.10	**8.30**	0.00	2.60	0.25	2.70	0.00	**30.0**	0.00	2.60	0.00	2.70	**94.2**
	0.5 m/s "pull"	0.10	**7.60**	0.00	2.60	0.50	2.70	0.05	**13.4**	0.00	2.60	0.35	2.70	**76.4**
	0.5 m/s "push"	0.10	**6.90**	0.00	2.60	0.30	2.70	0.00	**7.45**	0.00	2.60	0.00	2.70	**24.4**
Larger Tunnel	No vent.	0.10	**9.50**	0.70	3.00	1.25	3.90	0.00	**13.55**	0.25	3.45	1.30	4.00	**8.5**
	0.5 m/s "pull"	0.10	**8.65**	0.60	3.10	1.40	4.00	0.05	**12.25**	0.00	3.70	1.50	4.00	**12.7**
Obstacle: loader	No vent.	0.00	**4.50**	0.00	2.60	0.00	2.70	0.00	**30.0**	0.00	2.60	0.00	2.70	**360+**
	0.5 m/s "pull"	0.00	**3.30**	0.00	2.60	0.00	2.70	0.00	**3.40**	0.00	2.60	0.00	2.70	**11.1**
	0.5 m/s "push"	0.00	**3.65**	0.00	2.60	0.00	2.70	0.00	**8.95**	0.00	2.60	0.00	2.70	**19.4**
Leak on ground	No vent.	0.10	**15.30**	0.00	2.60	0.00	1.60	0.00	**22.30**	0.00	2.60	0.00	1.70	**10.4**
	0.5 m/s "pull"	0.10	**14.50**	0.00	2.60	0.00	1.60	0.05	**20.25**	0.00	2.60	0.00	1.70	**11.8**
Cavity	No vent.	0.10	**8.30**	0.00	2.60	0.25	2.70	0.00	**26.3**	0.00	2.60	0.00	3.70	**50.8**
	0.5 m/s "pull"	0.10	**7.60**	0.00	2.60	0.50	2.70	0.05	**9.20**	0.00	2.60	0.35	3.55	**30.5**
Wall rough.	No vent.	0.10	**8.05**	0.00	2.60	0.15	2.70	0.00	**20.50**	0.00	2.60	0.00	2.70	**67.5**
	0.5 m/s "pull"	0.10	**7.40**	0.00	2.60	0.40	2.70	0.05	**12.20**	0.00	2.60	0.15	2.70	**146.8**

In Figure 6, despite it showing contours starting at 2% hydrogen by volume, compared to the other scenarios, it shows that an obstacle completely changes the behavior of the hydrogen cloud. Most of the cloud accumulates behind the loader after hitting the obstacle instead of dispersing inside the mine opening. The two ventilation scenarios show a marked improvement over the no ventilation condition and as shown by Table 1 the effectiveness of "pull" ventilation in removing the hydrogen is greatly improved. However, under "push" ventilation high concentrations are seen to migrate to the floor and under the loader. On the other hand the average concentration of hydrogen in the cloud for the no ventilation and "push" case can be much higher, which will result in higher overpressures if ignited. For the "pull" case, although it shows a lower concentration than the other two, the size of the cloud in the vicinity of the leak, i.e. up to 1 m, occupies a greater percentage of that space increasing the potential for an ignition in that region.

While not shown in these results, in the case of a small uncontrolled release (m_{fr} = 0.007 kg/s), it was found that both "pull" and "push" ventilation are sufficient to prevent any accumulation of hydrogen inside the tunnel.

An interesting phenomenon was also observed in the scenario with an obstacle under no ventilation: after 360 sec of simulation, the hydrogen cloud at 4% molar fraction was still slowly oscillating at the ceiling from wall to wall but steadily dispersing itself. With the obstacle, the dispersion of the cloud slowed down significantly because a large portion of the initial momentum of the hydrogen jet is lost when hitting the loader.

As expected, when the leak exit is positioned near the ground, the extent of the cloud is much larger. On the other hand, because a greater portion of the cloud is exposed to the surrounding atmosphere and because its overall concentration distribution is lower, the time it takes to dissipate the cloud below the LFL concentration is much shorter than when the leak is positioned in the middle of the wall.

In the scenario with a cavity, it was determined that no amount of hydrogen above 4% molar fraction remained inside the cavity for more than a minute. While in the scenario with a custom wall roughness, with ventilation, small pockets of hydrogen near the LFL concentration lingered inside the small cavities along the walls for a little more than 2 minutes.

5.0 COMBUSTION RESULTS

The combustion simulations were also performed in two stages. First the hydrogen was released in the domain for 3 sec, then the release is stopped and the hydrogen is ignited. For each combustion case the ignition position is set inside the stoichiometric concentration region of the cloud (30% (vol)) along the center axis of the tunnel (y = 1.3 m). For most simulation scenarios, this corresponded to x = 1.65 m, y = 1.3 m and z = 1.35 m. For all cases the ventilation is stopped right before igniting the cloud following Gexcon recommendation for explosion simulations [11].

Table 2.Maximum combustion overpressure in the domain and on the monitor points for the scenarios with and without ventilation.

Scenarios		Maximum overpressure in the domain (barg)	Maximum overpressure at the monitor points (barg)
Default Tunnel	No ventilation	0.1086	0.1082
	0.5 m/s “pull”	0.1777	0.1770
	0.5 m/s “push”	0.1506	0.1502
Larger Tunnel	No ventilation	0.0355	0.0354
	0.5 m/s “pull”	0.0516	0.0374
Obstacle: loader	No ventilation	1.0004	0.9975
	0.5 m/s “pull”	0.5773	0.5732
	0.5 m/s “push”	0.3818	0.3811
Leak on ground	No ventilation	0.0890	0.0888
	0.5 m/s “pull”	0.1063	0.1059
Wall roughness	No vent.	0.1550	0.1542
	0.5 m/s “pull”	0.1984	0.1966

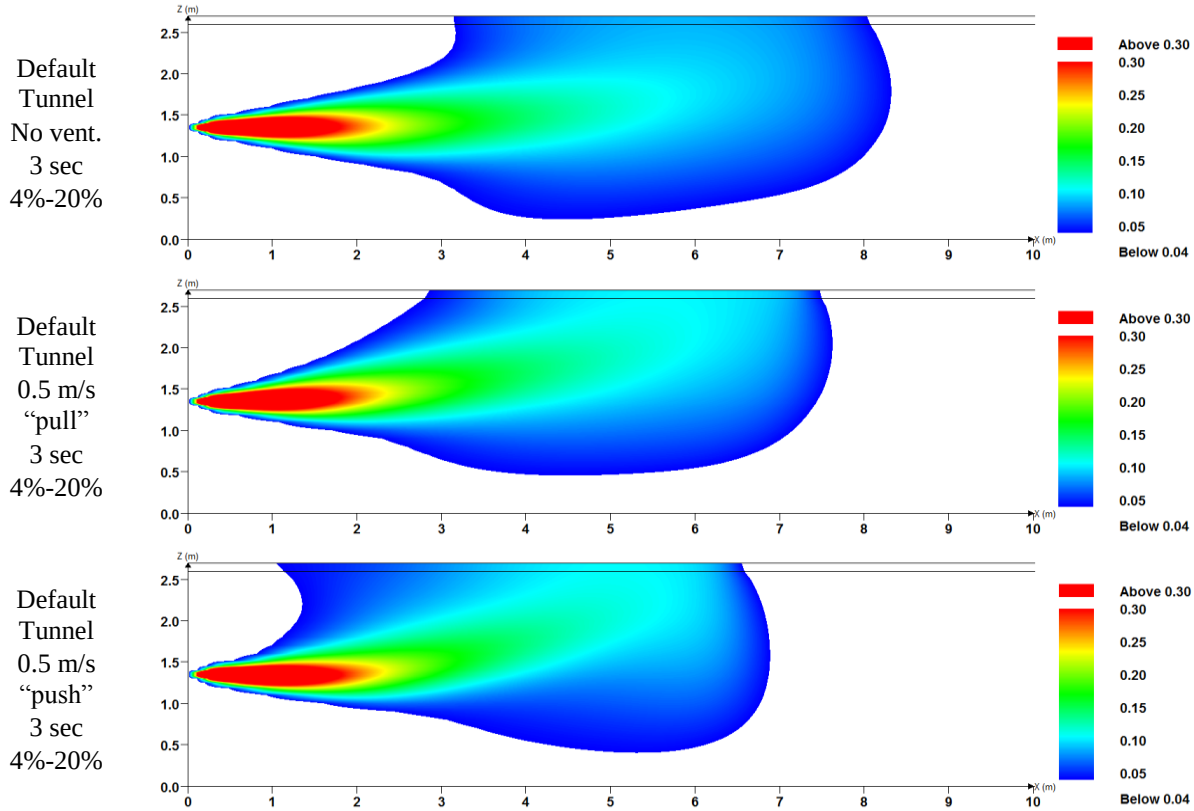

Figure 5. Hydrogen concentration envelope profiles (up to 30% (vol), in red) from the lower flammability limit contour (4% (vol), in blue) along the jet direction (Y = 1.3 m) for the full leak scenarios in an empty tunnel.

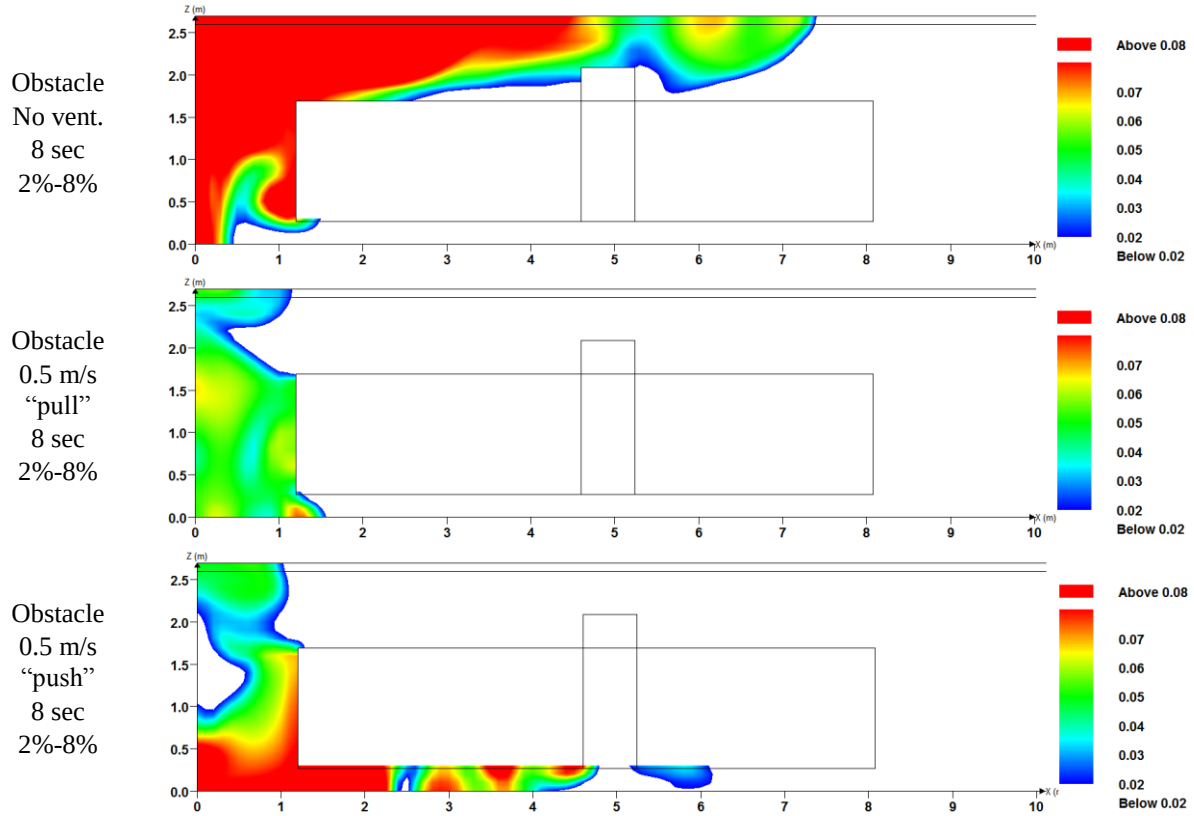

Figure 6. Hydrogen concentration envelope profiles (up to 8% (vol), in red) from half the lower flammability limit contour (2% (vol), in blue) along the jet direction (Y = 1.3 m) for the full leak scenarios with an obstacle.

The maximum overpressures measured in the domain as well as at the monitor points for each scenario are given in Table 2. The monitor points are positioned every 5 m at a heights of 0 m, 0.3 m, 0.6 m and 1.5 m from the ceiling along the center axis of the tunnel (y = 1.3 m).

As shown by the results in Table 2, overpressures are marginally higher for the scenarios with "pull" and "push" ventilation than for the scenarios without ventilation. As explained above, the lower concentration part of the hydrogen cloud is pushed back into the higher region by the ventilation, raising the overall concentration of the cloud near the release point. This results in stronger overpressures. The phenomenon is more pronounced with the "pull" ventilation. The lowest overpressures are seen with the larger tunnel. Increasing the size of the tunnel reduces confinement; consequently the overpressures are significantly lower. On the other hand, adding an obstacle increases confinement. Consequently much higher overpressures are observed with the loader in place: up to 10 times higher in the case without ventilation. Since the hydrogen cloud is being confined behind the loader, this greatly increases the average concentration in the cloud and results in stronger overpressure. Even though "pull" ventilation is more efficient at purging the hydrogen cloud outside the domain, when ignited at 3 sec, the "push" ventilation yielded the lowest overpressures.

A larger cloud will not necessarily result in a larger explosion. This was seen with the leak positioned near the ground. Since the cloud is more stretched and the same amount of hydrogen released, the overall concentration in the cloud is lower which results in a lesser explosion.

Finally to assess the effect of the ignition delay on the combustion results, it was varied in step of 0.025 sec until ignition was no longer possible. When varying the ignition delay the ignition position is kept constant at x = 1.65 m, y = 1.3 m and z = 1.35 m. As shown by the results in Table 3, overpressures are very dependent on the ignition delay. An ignition delay equal or greater than 0.175 sec is enough to prevent ignition.

Table 3. The ignition delay was varied from 3.000 sec to 3.175 sec for the scenario with 0.5 m/s "pull" ventilation and a leak duration of 3 sec inside an empty tunnel. The ignition position was fixed at X = 1.65 m, Y = 1.3 m and Z = 1.35 m.

Ignition delay (sec)	Max OP domain (barg)	Max OP gauges (barg)	Difference
3.000	**0.178**	**0.177**	**0%**
3.025	0.168	0.167	-6%
3.050	0.159	0.159	-10%
3.075	0.153	0.152	-14%
3.100	0.147	0.147	-17%
3.125	0.127	0.126	-29%
3.150	0.079	0.079	-56%
3.175	0.000	0.000	-100%

6.0 CONCLUSIONS

Based on the results in this study, it is difficult to derive a definitive conclusion on which ventilation strategy is optimal. "Push" and "pull" differ in the structure of their flow fields in the tunnel (Figure 2, Figure 4), the velocities being larger close to the exhaust vent in a "pull" scenario. While the "push" ventilation appears to be more effective for short releases, this seems to be due to enhanced dispersion through additional air circulation in the tunnel, rather than evacuation of hydrogen from the tunnel which is provided by the "pull" ventilation. This hypothesis seems to be particularly supported by the test with an obstacle as illustrated in Figure 6. This figure shows that at the 8 sec mark, the "pull" ventilation achieved a significantly smaller H_2 flammable cloud than the "push" ventilation. Also, the drag of hydrogen underneath the loader by "push" ventilation is clearly observed. In any case, for all short release scenarios both the "pull" and "push" ventilation running at 0.5 m/s were able to disperse

the hydrogen cloud below the lower flammability limit concentration in less than 3 minutes. When considering the time it takes for the 4% cloud to dissipate, it must be kept in mind that any ignition event must occur within that time. If no ignition possibility exists during that time, then the system can be considered safe according to the simulations.

Ultimately further research will have to be undertaken to refine the results in the light of risk levels and mitigation. Other options will also need to be considered, such as both "push" and "pull" scenarios, to offer the lowest risk and highest safety for workers for the range of possible sudden accidental releases as well as slow hydrogen leak build-ups.

For the combustion simulations, the worst case scenario was assumed: ignition was set inside the 30% molar fraction envelop (region of highest ignition probability) right after the leak stopped (worst possible time). Overpressures of up to 1 barg were seen in the case where a loader was present without any ventilation. For the scenarios with the ventilation, the overpressure went down by 40% to 0.6 barg for the "pull" ventilation and by 60% to 0.4 barg for the "push" ventilation. Finally when considering how the overpressures depend on the ignition delay, while keeping the ignition position constant, it was found that an ignition delay of more than 0.175 sec, prevents the explosion from occurring.

ACKNOWLEDGEMENTS

The authors would like to thank the Hydrogen Mine Introduction Consortium members (Air Liquide, Barrick Gold, Goldcorp, Hydro-Quebec, IAMGOLD, Vale, Xstrata Nickel Raglan Mine) for their project support.

REFERENCES

1. Strebig, K. & Waytulonis, R., 1987, "The Bureau of Mines' hydrogen powered mine vehicle," *SAE Technical Paper 871678*, 1987, doi:10.4271/871678.
2. Hardcastle S.G., Kocsis C., Bétournay M. & Barnes D., 2004. The benefits of replacing the diesel engine with a fuel cell in underground mining production equipment, *Proc. 10th U.S./N. American Mine Ventilation Symposium 2004*, pp 397-407, Balkema, ISBN 90-5809-633-5.
3. Righettini, G. & Mousset-Jomes, P., 2004, Ventilation savings with fuel cell vehicles, *Proc. 10th U.S./N. American Mine Ventilation Symposium 2004*, pp 433-443, Balkema, ISBN 90-5809-633-5.
4. Houf, W., Winters, W. & Evans, G., 2008, Approximate Inflow Conditions for Subsonic Navier-Stokes Computations of Under-Expanded Jets, Private communication. Sandia National Laboratories Livermore, CA 94550.
5. Middha, P., Hansen, O.R. & Storvik, I.E., 2009, Validation of CFD-model for hydrogen dispersion, *Journal of Loss Prevention in the Process Industries*, 22(6), pp 1034-1038, ISSN 0950-4230.
6. Baraldi, D., Kotchourko, A., Lelyakin, A., Yanez, J., Middha, P., Hansen, O.R., Gavrikov, A., Efimenko, A., Verbecke, F., Makarov, D., and Molkov, V., 2009, An inter-comparison exercise on CFD model capabilities to simulate hydrogen deflagrations in a tunnel, *International Journal of Hydrogen Energy*, 34(18), pp 7862-7872, ISSN 0360-3199.
7. Middha, P., Hansen, O.R., Grune, J. & Kotchourko, A., 2010, CFD calculations of gas leak dispersion and subsequent gas explosions: Validation against ignited impinging hydrogen jet experiments, *Journal of Hazardous Materials*, 179(1-3), pp 84-94, ISSN 0304-3894.
8. Venetsanos, A.G., Papanikolaou, E., Delichatsios, M., Garcia, J., Hansen, O.R., Heitsch, M., Huser, A., Jahn, W., Jordan, T., Lacome, J.-M., Ledin, H.S., Makarov, D., Middha, P., Studer, E., Tchouvelev, A.V., Teodorczyk, A., Verbecke, F. & Van der Voort, M.M., 2009, An inter-comparison exercise on the capabilities of CFD models to predict the short and long term distribution and mixing of hydrogen in a garage, *International Journal of Hydrogen Energy*, 34(14), pp 5912-5923, ISSN 0360-3199.
9. Jordan, T., García, J., Hansen, O., Huser, A., Ledin, S., Middha, P., Molkov, V., Travis, J., Venetsanos, A., Verbecke, F. & Xiao, J., 2007, Results of the HySafe CFD Validation Benchmark SBEPV5, *Proc. 2nd International Conference on Hydrogen Safety*, San Sebastian Spain, 11-13

September, 2007.
10. Mattei, N., Schiavetti, M., & Carcassi, M.N., 2011, Experimental studies on wind influence on hydrogen release from low pressure pipelines, *International Journal of Hydrogen Energy*, 36(3), pp 2414-2425, ISSN 0360-3199.
11. FLACS, 2011, Version 9.1 User's guide, Gexcon, April 2011.